Sensors and Actuators B 252 (2017) 973–982

Contents lists available at ScienceDirect

Sensors and Actuators B: Chemical

journal homepage: www.elsevier.com/locate/snb

Fat taste detection with odorant-binding proteins (OBPs) on screen-printed electrodes modified by reduced graphene oxide

Yanli Lu[a,b], Yixuan Huang[a], Shuang Li[a,b], Qian Zhang[a,b], Jiajia Wu[a,b], Zhongyan Xiong[a], Lingxi Xiong[a], Qianqian Wan[a], Qingjun Liu[a,b,*]

[a] Biosensor National Special Laboratory, Key Laboratory for Biomedical Engineering of Education Ministry, Department of Biomedical Engineering, Zhejiang University, Hangzhou, 310027, PR China
[b] Collaborative Innovation Center of TCM Health Management, Fujian University of Traditional Chinese Medicine, Fuzhou, 350122, PR China

ARTICLE INFO

Article history:
Received 8 March 2017
Received in revised form 7 June 2017
Accepted 14 June 2017

Keywords:
Fat taste
Gustatory biosensor
Odorant-binding proteins (OBPs)
Cyclic voltammetry (CV)
Reduced graphene oxide

ABSTRACT

Except for the widely accepted taste primaries—sour, sweet, bitter, salty, and umami, increasing evidence indicated that the existence of a taste modality responsive to fat. Based on the hydrophobic nature of dietary fats, a new kind of gustatory biosensor with odorant-binding proteins (OBPs) modified screen-printed electrodes was designed for sensing the "fat taste". Through electrochemical reduction, graphene oxide was modified on the carbon electrodes to form a sheet that comprised graphene domains with residual oxygen-containing functional groups, which could increase the electrode conductivity and be used for protein immobilization. For fat taste sensing, taste substances of medium- and long-chain fatty acids, such as lauric acid, linoleic acid, and docosahexaenoic acid, were detected through cyclic voltammetry. Moreover, the sensor showed high affinities to medium- and long-chain fatty acids comparing to the tastants of other five primaries tastes. The gustatory biosensor offered a powerful analytic technique for detecting fat taste substances, which seem to be an alternative to labor-intensive and time-consuming cell-based assays or animal experiments. Furthermore, it could be treated as the sensory evaluation panels for food and beverage industry, and even for disease managements.

1. Introduction

For different organisms, especially human beings, taste (or flavor perception) is a form of direct chemoreception, which is responsible for helping intake of essential and scarce nutrients, while preventing the consumption of toxic and indigestible substances [1,2]. Utilizing the detection property of taste sense, different sensors were established to perceive and discriminate various taste substances [3,4]. In the taste researches, it was widely accepted that the basic taste qualities were composed of sour, sweet, bitter, salty, and umami. Thus, perception and recognition of those basic taste qualities have long been the center issues, which showed great potential commercial prospects in food safety, pharmaceutical industry, and environment monitoring [5–8]. With the developments of lipid/polymer membrane, and tissue- and cell-based biosensors, many achievements have been made in the taste detection [3,9]. However, the sensitivity and selectivity still should be improved for the bioinspired systems.

In biology systems, studies have suggested that odorant-binding proteins (OBPs) were in charge of binding small hydrophobic or lipophilic molecules to enhance their aqueous solubility, and transporting them to the receptors on sensory cells [10–12]. As a kind of extracellular proteins, OBPs have been found in different organs of both insects and mammals with specific binding functions [13,14]. As a natural protein scaffold for recognition of hydrophobic molecules, various OBP-based biosensors have been developed for hydrophobic molecule sensing as smell sensors [15–17]. Beyond mimicking organisms' sensing system, however, nature sensing system inspired artificial sensors to do more with less. For human OBPs, mainly including OBP II a and OBP II b that belong to the lipocalin superfamily, they were not only identified in nasal epithelia to make sense of smell, but also were found as the extracellular carriers and scavengers of lipophilic ligands in several other important organs, such as salivary, lachrymal, prostate, and mammary glands [18,19]. Therefore, they might play important binding roles in these organs, which inspired us to develop novel sensors with specific sensing functions. Through investigating the ligand-binding spectrum of human OBPs, researchers found that OBP II

* Corresponding author at: Biosensor National Special Laboratory, Key Laboratory for Biomedical Engineering of Education Ministry, Department of Biomedical Engineering, Zhejiang University, Hangzhou, 310027, PR China.
E-mail address: qjliu@zju.edu.cn (Q. Liu).

http://dx.doi.org/10.1016/j.snb.2017.06.100
0925-4005/

a had high affinities to fatty acids [20,21], which might offer an platform to detect fat-soluble substances for evaluating fat taste.

Increasing evidence indicated that dietary fat (lipid) was perceived not only by texture perception, retronasal olfactory, and post-ingestive cues, but also through taste sensing in the oral cavity [22–24]. With implicated multiple candidate receptors and ion channels for fat taste substances have been detected, considerable studies from rodent and human raised the possibility for the hypothesis that oral fat exposure elicited a unique taste sensation, which might be the sixth taste modality: fat taste [25–27]. Based on the chemosensory and nutrition researches, fatty acids with different length of carbon chains might be treated as different taste stimulus. Short-chain fatty acids stimulated a sensation similar to the taste of sour, such as carboxylic acids, while medium- and long-chain fatty acids have a relatively diverse sense that caused by different alkyl chain lengths [28]. Similar to other tastes, fat taste also played important roles in regulating the intake of oral nutritions. Especially, the taste sensitivity to some types of fat taste substances had been closely related to the predisposition of overweight or obesity in both animals and humans [29–31]. Therefore, as fat taste was closely related to human health, fat taste and fat tastes substances detection should be further explored.

With the properties of high surface area, excellent electrical conductivity and strong mechanical strength, graphene was treated as an ideal electrode material for biosensors. Synthesis of high quality graphene sheets in large scale from graphene oxide through electrochemical reduction was fast and green [32,33]. Through electrochemically reduced, considerable numbers of oxide groups of graphene oxide were removed while the extensive conjugated sp^2 carbon network was restored. Therefore, the electrical conductivity of the modified electrode increased due to the modified reduced graphene oxide (rGO) layers. Meanwhile, residual oxygen functionalities (—OH and —COOH) of the rGO film could be further used for protein immobilization. The obtained compact rGO films with a high mechanical integrity and interconnected networking structure were important for bio-sensing.

In this study, based on the taste perception and the hydrophobic nature of dietary fats, a new kind of gustatory biosensor with OBPs modified screen-printed electrodes was fabricated for sensing fat taste. Through electrochemical reduction, reduced graphene oxide was immobilized on the carbon electrodes directly, to form a sheet comprised graphene domains interspersed with residual oxygen-containing function groups. In the experiments, different taste substances of docosahexaenoic acid, linoleic acid, lauric acid, and acetic acid were tested with cyclic voltammetry to evaluate the binding affinities and speculate their taste stimuli. The biosensor offered a new way for detecting and evaluating fat taste, which might hold great implications for food product choice and development, and even for clinical practices.

2. Materials and methods

2.1. Recombinant human OBP and reagents

Based on that human OBP II a had a high affinity to fat taste substances of fatty acids [16,20], the expression and purification of the active recombinant OBP II a were cloned from the full-length cDNA of human in Wuhan Huamei Biotech Co., Ltd (China). Briefly, a DNA sequence encoding the OBP II a was expressed with a poly histidine tag at the C-terminus in the host cells of Escherichia coli. After harvesting the host cells, the crude cell extracts, pellet and supernatant were analyzed by sodium dodecyl sulfate-polyacryl amide gel electrophoresis (SDS-PAGE) [16]. The recombinant OBP II a consisted of 170 amino acids and predicted a molecular mass of 32 kDa. The protein was suspended at 100 μg/ml in phosphate buffered saline (PBS, pH = 7.4) and saved under 4 °C for the following experiments.

Graphene oxide (GO) was obtained from Nanjing XFNANO Materials Tech Co., Ltd. (China). N-hydroxysuccinimide (NHS) and 1-ethyl-3-(3-dimethylaminopropyl) carbodiimide (EDC) were dissolved in 2-(4-Morpholino) ethanesulfonic acid (MES) for protein immobilization. Fat taste substances of docosahexaenoic acid, linoleic acid, and lauric acid were prepared into different concentrations, 10^{-9} mg/ml, 10^{-8} mg/ml, 10^{-7} mg/ml, 10^{-6} mg/ml, 10^{-5} mg/ml, 10^{-4} mg/ml. Acetic acid, glucose, cycloheximide, sodium chloride, and L-monosodium glutamate were respectively used as the typical tastants of sour, sweet, bitter, salty, and umami, the tested concentrations of which were also prepared into 10^{-9} mg/ml, 10^{-8} mg/ml, 10^{-7} mg/ml, 10^{-6} mg/ml, 10^{-5} mg/ml, 10^{-4} mg/ml. Potassium ferricyanide/ferrocyanide, $K_4Fe(CN)_6/K_3Fe(CN)_6$ (1:1) solution containing 0.1 M KCl was employed as redox couple in aqueous solution for electrochemical measurements to get a stable and symmetric peak currents in the cyclic voltammetry (Fig. A1 in the appendix). Sodium sulfate (Na_2SO_4) was prepared into 0.5 M with ultrapure water, used as the solvent in electrochemical reduction. All of the chemical reagents above were of analytical grade and purchased from Sigma-Aldrich, USA.

2.2. Apparatus

All of the electrochemical experiments were performed on CH Instruments 660E electrochemical analyzer (CH Instruments, Inc.). The surface morphology of graphene oxide and electrochemical reduced graphene oxide (rGO) was evaluated by scanning electron microscope (SEM, Philips XL-30 ESEM) at an accelerating voltage of 15 kV. Screen-printed electrodes provided by GSI Technologies, LLC (Burr Ridge, IL, USA), were used for all of the electrochemical experiments. The electrodes were printed on 3 cm × 1 cm polyethylene glycol terephthalate substrate, each of which consisted of a silver electrode as reference electrode, a carbon electrode as counter electrode, and a carbon electrode (3 mm in diameter) as working electrode (Fig. 1a). The electrical connects on bottom of the electrodes were also made of silver and could be linked to the electrochemical workstation with a self-designed socket.

2.3. Electrochemical reduction of graphene oxide on the screen-printed electrodes

In order to increase conductivity of screen-printed electrodes and immobilize sensing proteins, graphene oxide was reduced on the working electrodes through electrochemical method. After dispersing graphene oxide in ultrapure water, five different concentrations (1 mg/ml, 2 mg/ml, 3 mg/ml, 4 mg/ml, and 5 mg/ml) of the homogeneous graphene oxide dispersion could be made under ultrasonication for 2 h. Before modified with graphene oxide, the bare electrodes were thoroughly rinsed with ultrapure water, and then successive cyclic voltammetric sweeps were conducted until the steady curve appeared. It was scanned in a potential range from 1.0 V to −1.0 V with the scan rate and sensitivity were 50 mV/s and 10^{-4} A/V, respectively.

As the circular working electrode's diameter was 3 mm, a drop about 3 μl graphene oxide dispersion was put onto the cleaned carbon working electrodes to produce a flat membrane of graphene oxide. After the graphene oxide dispersion drying at room temperature, an electrochemical reduction process was applied to directly obtain rGO modified electrodes. After graphene oxide was reduced on the screen-printed electrodes via electrochemical reduction, the electrodes were thoroughly rinsed with ultrapure water to obtain the rGO modified electrodes for the following testes.

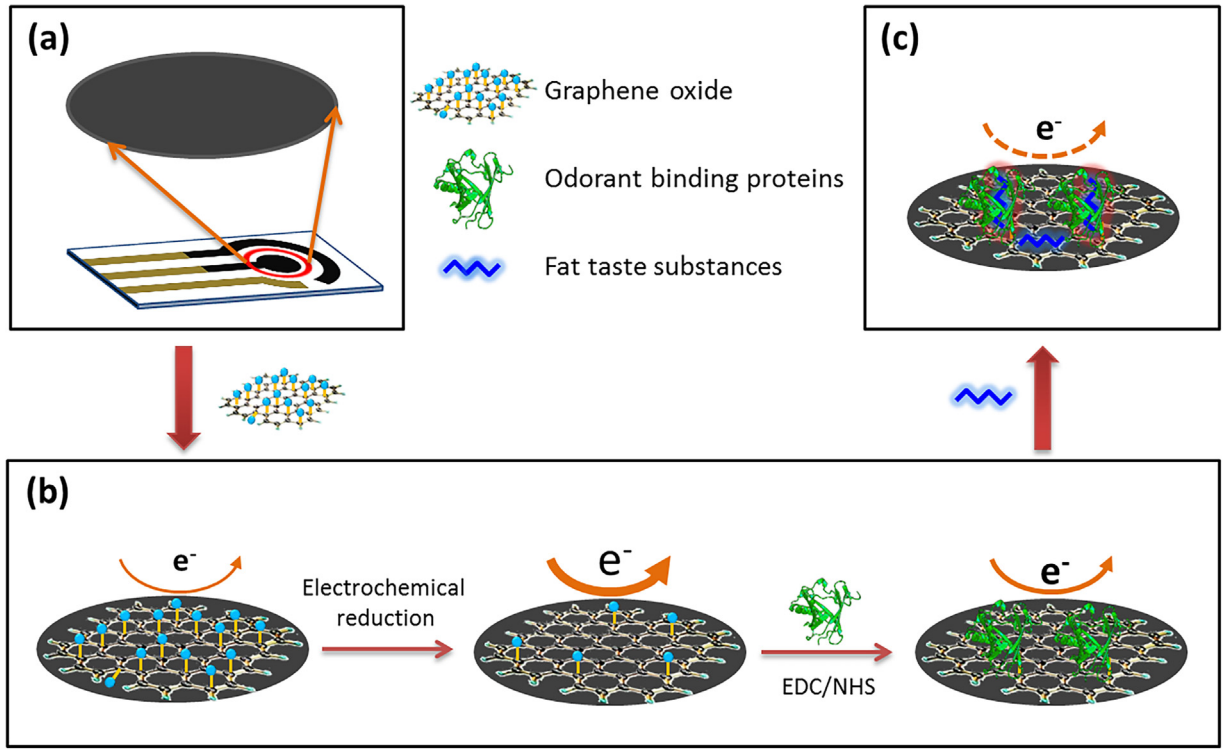

Fig. 1. Schematic diagram of developing the electrochemical gustatory biosensor. (a) Screen-printed electrodes that containing a working electrode, a reference electrode, and a counter electrode. (b) Stepwise preparation of the electrochemical reduction of graphene oxide and OBP-modified electrodes. (c) Interactions between fat taste substances and OBPs changed currents of cyclic voltammetry on the electrodes.

2.4. Immobilization of OBPs on the rGO modified electrodes

Compared to physical adsorption, and cross-lining with aromatic ring based linker or diazonium salt that used for immobilizing OBPs, rGO could greatly improve the conductivity of the working electrodes, which increased the sensitivity of the biosensors. Meanwhile, with the help of residual carboxyl groups of reduced graphene oxide, proteins could be immobilized on the electrodes through covalent bonding. In this experiment, OBP II a were covalently attached to the electrodes through EDC/NHS chemistry. EDC and NHS solutions were prepared in 0.1 M MES buffer (pH = 6, contained 0.5 M sodium chloride), respectively. To activate the carboxyl groups of the rGO, the electrodes were immersed in the mixed solution of equal volume (50 μl) of EDC (2 mM) and NHS (5 mM) for 15 min. After pH of the mixed solution was increased to 7.4 with sodium bicarbonate, 50 μl of OBP II a solution was added into the mixed solution. Then, putting the electrodes at 4 °C for 2 h to allow forming the amide linkages (Fig. 1b). After that, the electrodes were thoroughly rinsed with PBS buffer to remove the unreacted EDC/NHS solutions and unbound OBP II a. Cyclic voltammetry testes were scanned in the potential range from 1.0 V to −1.0 V. The OBP-modified electrodes were saved under 4 °C for the following fat taste detection (Fig. 1c). All of the above processes were performed at room temperature (22 ± 2 °C).

2.5. Electrochemical measurements

Docosahexaenoic acid, linoleic acid, and lauric acid were tested as the tastants of fat taste, which were prepared for different concentrations of 10^{-9} mg/ml, 10^{-8} mg/ml, 10^{-7} mg/ml, 10^{-6} mg/ml, 10^{-5} mg/ml, and 10^{-4} mg/ml. In the experiment, 100 μl of the fat taste substances at different concentrations were added to a designed cell containing 450 μl $Fe(CN)_6^{3-/4-}$ (1:1). The cell was fabricated with a volume of 650 ± 20 μl. The detailed information was showed in the appendix (Fig. A2). For electrochemical detection of these tastants, the potential ranges were set from 1.0 V to −1.0 V with the scan rate was 50 mV/s. After each measurement, the tested solutions were removed out of the reaction chambers, and the chambers were thoroughly rinsed with ultrapure water. Meanwhile, the OBP-modified electrodes were immersed in PBS buffer for 5 min to eliminate the residual tastants for the recovery of the proteins. Parallel experiments for these fat taste substances were tested at least three times.

As the typical tastants for sour, sweet, bitter, salty, and umami, substances of acetic acid, glucose, cycloheximide, sodium chloride, and L-monosodium glutamate were respectively tested with the protein-based biosensor. The experimental steps of these tastants were the same as that of fat taste detection. All of the electrochemical measurements were also performed at room temperature (22 ± 2 °C).

3. Results

3.1. Electrochemical reduction of graphene oxide on the electrodes

Reduced graphene oxide was chosen not only for enhance conductivity of the electrodes, but also for immobilizing the sensing proteins. The relationships between concentrations of GO solution and the sensitivity were systematically characterized through electrochemical sensing. The electrical conductivity of the modified electrodes increased with the concentrations of GO increasing (Fig. A3). However, when the concentration of GO solution was higher than 3 mg/ml, the layer of GO was crackly in the reduction process. Therefore, we chose 3 mg/ml as the optimal concentration in forming a homogeneous reduced GO layer on the surface of electrodes. After the graphene oxide dispersion drying at room temperature, an electrochemical reduction process was applied to

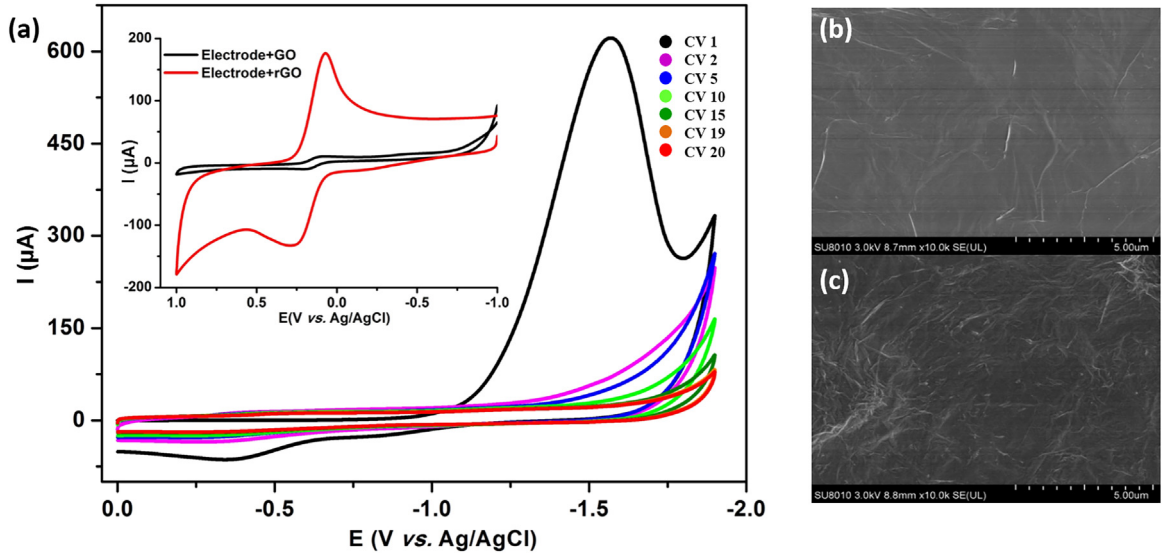

Fig. 2. Reduction and characterization of graphene oxide (GO) on the electrode. (a) Seven typical cyclic voltammograms of the electrochemical reduction of GO to reduced graphene oxide (rGO) in 0.5 M Na_2SO_4 at 50 mV/s. The inset was the cyclic voltammograms of the electrode that modified with GO and rGO. (b) SEM images of screen-printed electrodes modified with GO and (c) reduced graphene oxide (rGO).

directly obtain rGO modified electrodes by conducting successive cyclic voltammetric sweeps for 20 times in a potential range from 0 V to −1.9 V in the Na_2SO_4 solution (Fig. 2a). There was a large reduction peak current at −1.5 V in the first cycle with the starting potential of −1.0 V, which could be attributed to the reduction of the functional groups of the graphene oxide sheets, such as —OH, —COOH, and epoxides [34]. In the second cycle, the reduction current had a dramatic decline at negative potentials, especially that the reduction peak current was almost disappeared, indicating that the electrochemical reduction of graphene oxide was fast and irreversible. After 20 potential cycles that took about 26 min, there seemed to be no visible changes for the reduction currents, which indicated the fully reduction of graphene oxide. Meanwhile, from the cyclic voltammograms of potassium ferricyanide before and after the reduction of graphene oxide, we could find that the rGO increased the conductivity of the electrodes (Inset of Fig. 2a).

The surface morphologies of graphene oxide and rGO modified electrodes were investigated by SEM. As shown in Fig. 2b, graphene oxide displays a relative smooth surface. After directly electrochemical reduction, rGO exhibits a rough surface with random crumple and wrinkles (Fig. 2c), which might cause by a decrease in the size of the in-plane sp^2 domains and a partially ordered crystal structure of the rGO [34,35]. All the characterizations verify the successful reduction of graphene oxide. The morphology of rGO was highly beneficial in maintaining large electroactive area of the electrodes for the following experiments.

3.2. Electrochemical characterization of the OBP-modified electrodes

Based on that the modification of different materials on electrode surface could perturb electron transfer kinetics of $Fe(CN)_6^{3-/4-}$, both cyclic voltammetry and electrochemical impedance were tested to further confirm that the graphene oxide and OBPs were successfully assembled on the electrodes. Fig. 3a shows the cyclic voltammograms of potassium ferricyanide at the bare screen-printed electrodes, rGO modified electrodes and, OBP-immobilized electrodes. It indicated that the assembly of rGO on the electrodes was accompanied by an increase in the currents, which showed that rGO modification improved the electrical conductivity of carbon electrodes. It was in accordance with the results of electrochemical impedance detection that the resistance of electrodes had a dramatic decline after modified with rGO (Inset of Fig. 3a). Subsequently, after immobilizing OBP II a onto the electrodes, electron transfer was blocked by formation of the organized layers, because it was more difficult for the redox to penetrate the protein layer into the conductive electrodes. With impedance of the system increased, the oxidation and reduction peak currents obviously decreased by 50 μA in comparison with that of rGO modified electrodes. These results suggested that the rGO and OBP II a had been successfully immobilized onto the electrodes for fat taste sensing. To investigate the mechanism of the electrochemical process taking place on the sensor surface, the biosensor in 5 mM $[Fe(CN)_6]^{3-/4-}$ at different scan rates in the range of 10–100 mV/s was tested. As shown in the inset of Fig. 3b, the plot of the anodic and cathodic peak currents versus square root of the scan rate showed linear response over the range of the studied scan rates, with correlation coefficients of 0.9900 and 0.9989, respectively. This is the characteristic of a diffusion controlled electrochemical process on the biosensor surface.

3.3. Electrochemical sensing of fat taste substances

As the sensing membrane, OBPs could interact with different fat taste substances. The redox pair of ferricyanide/ferrocyanide, $Fe(CN)_6^{3-/4-}$, was treated as valuable tool for testing the kinetic barrier of the interface of solution and solid electrode. The fatty acids bound to OBPs could change the electrical conductivity of the proteins, which be characterized by changes of the reduction or oxidation peak currents of $Fe(CN)_6^{3-/4-}$. To investigate the specific binding between linoleic acid and OBP II a, cyclic voltammograms of linoleic acid at different concentrations from 10^{-9} mg/ml to 10^{-4} mg/ml were also detected without redox pair of $Fe(CN)_6^{3-/4-}$ (Fig. A4). There was no observable reduction or oxidation peaks for the detected molecules. Therefore, the redox pair was chosen to investigate conditions of the electrode surface.

With an 18-carbon chain, linoleic acid is a long-chain polyunsaturated fatty acid. Moreover, it belonged to the family of essential fatty acids, which meant that it was essential in the daily diet as human body cannot synthesize it *in vivo* [36]. Based on the studies that humans were more sensitive to the taste of linoleic acid [37,38], it was firstly chosen as the oral recognition of dietary fats in our

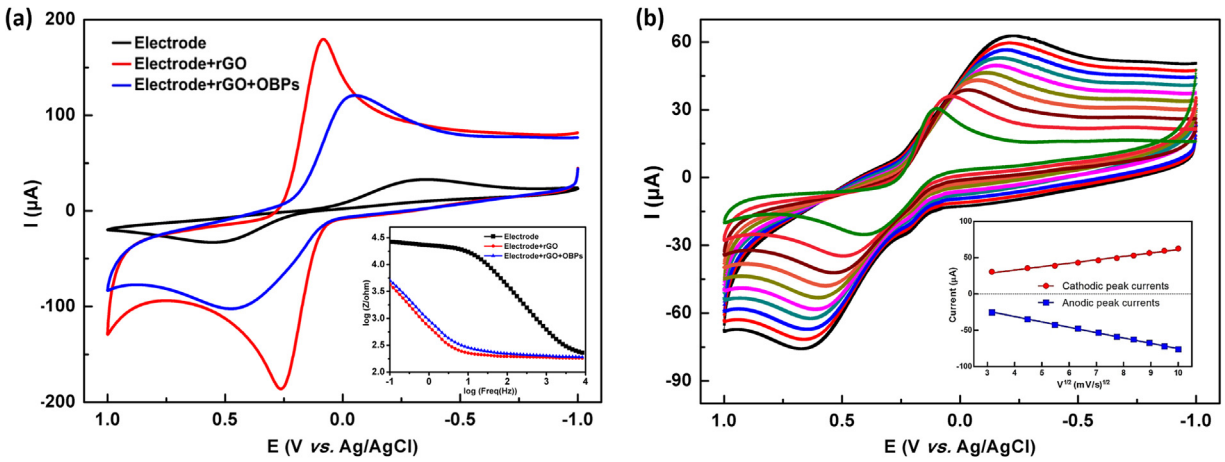

Fig. 3. Electrochemical characterization of the developed biosensors. (a) Cyclic voltammograms of reduced graphene oxide (rGO) and OBPs immobilized on the electrode. The inset was the electrochemical impedance plots of rGO and OBPs immobilized on the electrode. (The blank line: screen-printed electrode, the red line: rGO modified electrode, the blue line: OBPs immobilized on rGO modified electrode). (b) Cyclic voltammograms of the modified electrode under different scan rates (from inner to outer): 10, 20, 30, 40, 50, 60, 70, 80, 90, and 100 mV/s in 5 mM $Fe(CN)_6^{3-/4-}$ solution. Inset: anodic (blue) and cathodic (read) peak currents showed linear relationships with square root of the corresponding scan rate ($v^{1/2}$) with correlation coefficients of 0.9900 and 0.9989, respectively. (For interpretation of the references to colour in this figure legend, the reader is referred to the web version of this article.)

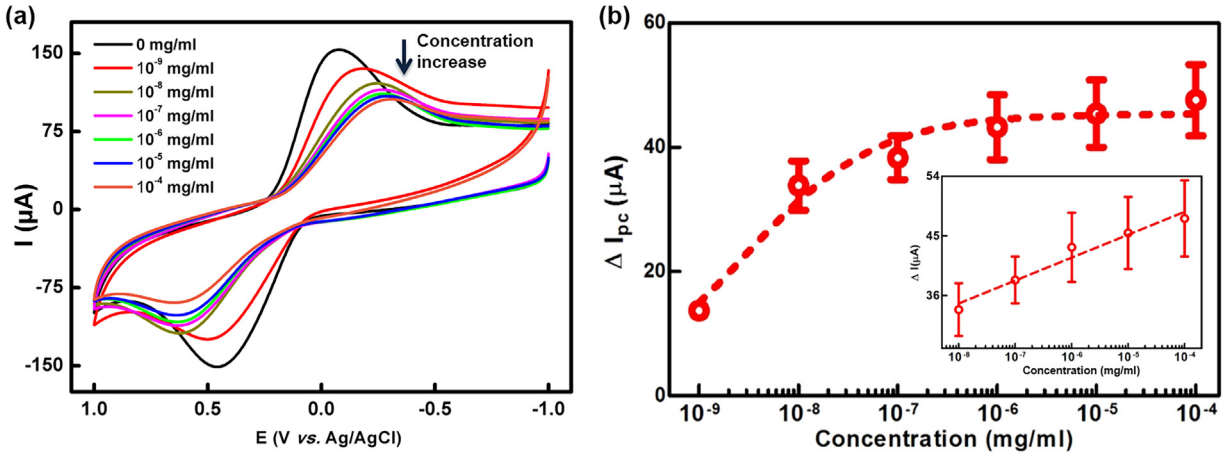

Fig. 4. Electrochemical detection of linoleic acid with the OBP-based biosensors. (a) Cyclic voltammograms of linoleic acid at different concentrations from 10^{-9} mg/ml to 10^{-4} mg/ml. (b) Hill plot obtained by the decrease of the cathodic peak currents from three replicated measurements. The inset was the linear calibration curve.

experiments. Different concentrations of linoleic acid were added into the detection cell that the electrodes were placed in to interact with human OBP II a. Then, the cyclic voltammetry measurements were conducted in presence of 5 mM $Fe(CN)_6^{3-/4-}$. Compared to the cyclic voltammograms of the test solution that without any fatty acids, the cathodic and anodic peak currents of linoleic acid decreased with the concentrations increasing (Fig. 4a). In order to determine the degree of cooperativity of linoleic acid binding to OBP II a, the relatively changes of the cathodic peak currents ($\triangle I_{pc}$) and anodic peak currents ($\triangle I_{pa}$) were calculated. As the similar responses were observed, the cathodic peak currents were chosen to analyze the binding interactions. The results of anodic peak currents ($\triangle I_{pa}$) were showed in the appendix (Fig. A5).

Through fitting the biochemical binding curve with the Hill equation, we got $\triangle I_{pc} = 45.4^*(X\ (/X + 2.95^*10^{-9}))^{0.65}$ for linoleic acid binding to the OBP II a based biosensor, where X represent the concentrations of linoleic acid (Fig. 4b). Moreover, the dissociation constant was calculated near 10^{-9} M, which showed a high binding affinity between linoleic acid and OBP II a. The Hill coefficient was about 0.65, which revealed that linoleic acid binding to OBP II a was a negatively cooperative binding form. That is, once one linoleic acid molecule was bound to OBP II a, its affinity for other molecules decreases.

Meanwhile, for the OBP-based biosensor, the linear working range of concentrations for linoleic acid was from 10^{-8} mg/ml to 10^{-4} mg/ml. The calibration curve could be described as $\triangle I_{pc} = 3.5^*X + 62.4$ ($r^2 = 0.9644$), where X was the logarithm of concentrations (Inset of Fig. 4b). The detection limit was near 10^{-10} mg/ml. To validate the interactions between linoleic acid and OBP II a, linoleic acid at different concentrations were also detected with the electrodes that without OBP II a (Fig. A6a). It showed that there was no obvious changes in both anodic and cathodic peak currents, which were lower than 10 μA (Fig. A6b). It suggested that interactions between linoleic acid and OBP II a could be sensitively detected by the OBP-based biosensor through CV measurements.

3.4. Analysis of different fat taste substances to the OBP-based biosensor

Short-chain fatty acids might stimulate a sensation similar to sour, however, the sensation might be changed as the chain length increased [22,28]. Therefore, another three different taste substances, docosahexaenoic acid, lauric acid, and acetic acid, were detected to explore whether short-, medium-, and long-chain fatty acids were unique in the sensation from each other.

Docosahexaenoic acid that contains 22 carbon atoms is one kind of polyunsaturated fatty acid, which might have a number of vital functions in vision, neuroprotection, and memory. Generally, it can be obtained from high-fat fish and marine mammals. Through CV measurements of docosahexaenoic acid at different concentrations, the interactions between docosahexaenoic acid and OBP II a were also proved. Similar to the results of linoleic acid, the anodic and cathodic peak currents of the CV measurements were also decreased with docosahexaenoic acid concentrations increasing (Fig. 5a). Though fitting tested data with the Hill equation, $\triangle I_{pc} = 56.2*(X/(X+8.51*10^{-12})^{0.23}$ was got for docosahexaenoic acid binding to OBP II a based biosensor (Fig. 5b). Meanwhile, the Hill coefficient was about 0.23, which indicated that docosahexaenoic acid binding to OBP II a was also showed a negatively cooperative binding form. Although the decreases of cathodic peak currents were a little bit larger than that of linoleic acid, the dissociation constant of OBP II a to docosahexaenoic acid (10^{-6} M) was lower than that of linoleic acid, which indicated a relatively lower affinity between docosahexaenoic acid and OBP II a. It was likely that the length of docosahexaenoic acid was longer than that of the binding cavity's size of OBP II a, which might lead to the folding of docosahexaenoic acid when binding to OBP II a [39–41]. Moreover, in the detected concentration ranges from 10^{-8} mg/ml to 10^{-4} mg/ml, cathodic peak current changes of docosahexaenoic acid were also showed a linear response, which could be represented by $\triangle I_{pc} = 3.4*X + 68.8$ ($r^2 = 0.9488$) (Inset of Fig. 5b). The detection limit was about $6*10^{-11}$ mg/ml.

For medium-chain fatty acids, lauric acid that is a saturated fatty acid with 12-carbon, was tested. Results showed that the anodic and cathodic peak currents of the CV measurements were also decreased with the increasing concentrations of lauric acid (Fig. 5c). The Hill equation of lauric acid binding to OBP II a was also calculated, $\triangle I_{pc} = 36.3*(X/(X+3.95*10^{-8}))^{0.27}$. The dissociation constant of OBP II a to lauric acid was about $5*10^{-5}$ M, which revealed its binding affinity was lower than that of linoleic acid and docosahexaenoic acid (Fig. 5d). As the Hill coefficient was about 0.27, lauric acid was also negatively cooperative binding to OBP II a. For lauric acid, the linear correlation curve could be represented by $\triangle I_{pc} = 3.9*X + 48.5$ ($r^2 = 0.9299$) with a detection limit was near 10^{-9} mg/ml (Inset of Fig. 5d). Moreover, compared to current changes of long-chain fatty acids, the current decreases of lauric acid at different concentrations were lower than 40 μA. It indicated that the interactions between lauric acid and OBP II a were lower, which had little effects on the OBP-based biosensor.

For short-chain fatty acids, they were kinds of volatile fatty acids that with less than 6 carbon atoms. Here, acetic acid was chose to be tested. Although the detected cathodic peak currents were also decreased (~20 μA), there was no differences between different concentrations (Fig. A7). Generally, acetic acid itself is actually a kind of short-chain fatty acids with two carbon atoms, which has a sour note that caused by the hydrogen ions in the solution. Therefore, the short-chain fatty acid had a quiet different influence on the immobilized proteins, which might be protein denaturation or related to the pH sensitive properties of OBP II a [42,43]. The OBP II a functionalized biosensor provided a potential approach not only for detecting medium- and long-chain fatty acids, but also for sensing and evaluating different fat tastes.

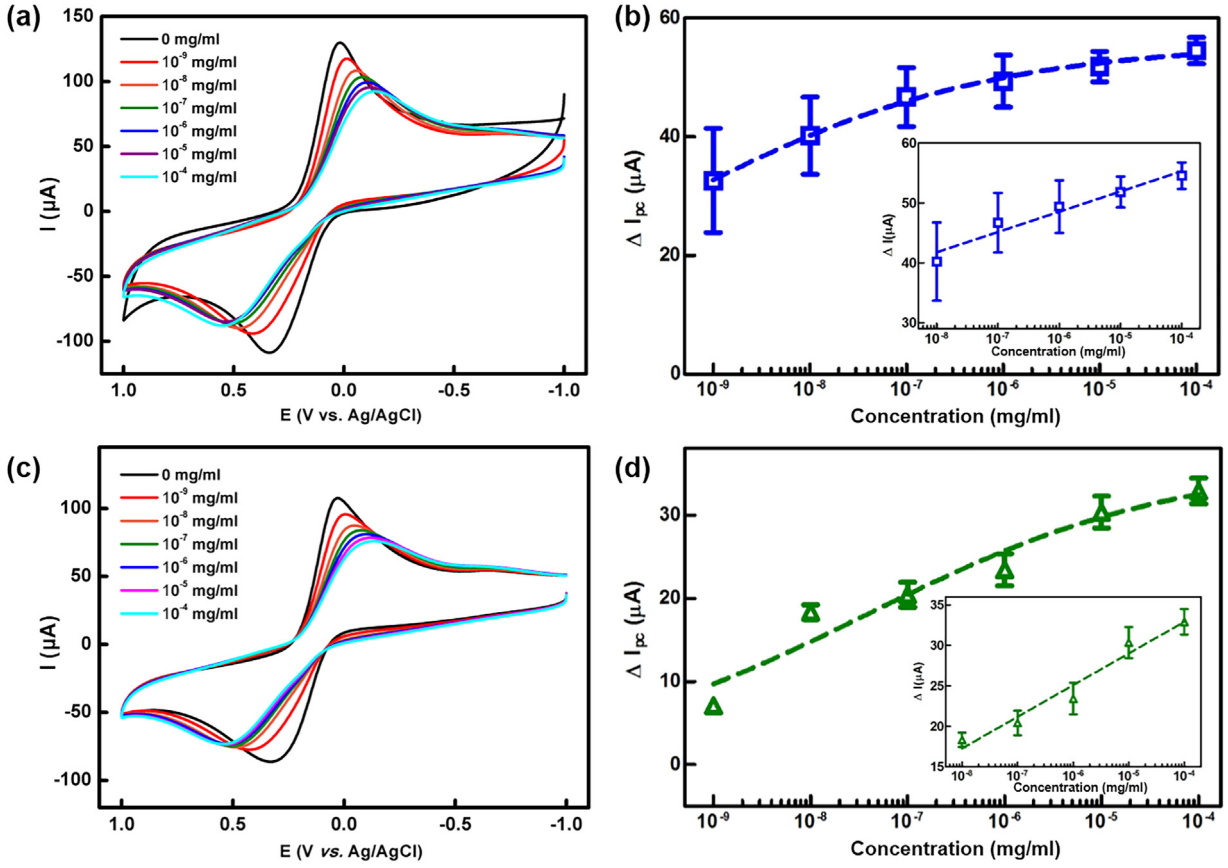

Fig. 5. Electrochemical detection of docosahexaenoic acid and lauric acid with the OBP-based biosensors. (a) Cyclic voltammograms of docosahexaenoic acid at different concentrations from 10^{-9} mg/ml to 10^{-4} mg/ml. (b) Hill plot of docosahexaenoic acid. The inset was the linear calibration curve. (c) Cyclic voltammograms of lauric acid at different concentrations from 10^{-9} mg/ml to 10^{-4} mg/ml. (d) Hill plot of lauric acid. The inset was the linear calibration curve.

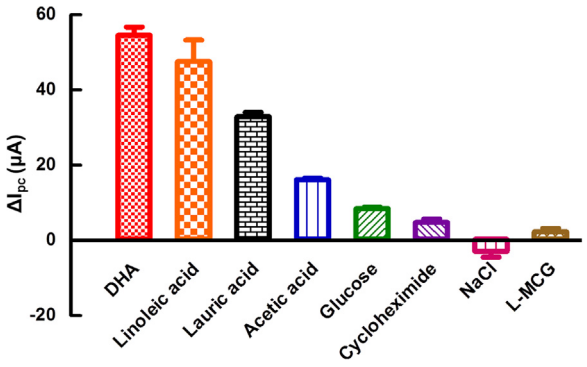

Fig. 6. Comparison of the cathodic peak current changes (ΔI_{pc}) of OBP-based biosensors to different fat taste substances of docosahexaenoic acid (DHA), linoleic acid, lauric acid, and other five different tastants, acetic acid (sour), glucose (sweet), cycloheximide (bitter), sodium chloride (NaCl, salty), and L-monosodium glutamate (L-MSG, umami) (n = 3).

3.5. Selectivity of different tastants to the OBP-based biosensor

Studies about fat taste suggested that medium- and long-chain fatty acids had a taste sensation that was distinct from other basic tastes—sour, sweet, salty, bitter, and umami [22,26,27]. Hence, a comparison between fat taste and other basic tastes was detected by the developed gustatory biosensor. For fat taste detection, the current changes that caused by fatty acids with a longer chain was much larger, which indicated that the binding affinities between OBP II a and long-chain fatty acids were stronger.

Although acetic acid belongs to fatty acids, it was widely accepted as one kind of sour tastants. Just as previous analysis, current changes of acetic acid at different concentrations were relatively low (~20 μA), which were difficult to distinguish the sour tastants. Moreover, the interactions of glucose (sweet), cycloheximide (bitter), sodium chloride (salty), and L-monosodium glutamate (umami) to OBP-modified electrodes were also tested. There were no obvious current changes in the cyclic voltammograms of these taste substances. In addition, to explore the interactions between OBP II a and all of the tastants, the cathodic peak current changes (ΔI_{pc}) of each tastant at 10^{-4} mg/ml were also calculated. As shown in Fig. 6, all of cathodic peak current changes of glucose, cycloheximide, sodium chloride, and L-monosodium glutamate were lower than 10 μA. It suggested that the interactions between OBP II a and these four tastants were so little that could not be detected by the biosensor. Thus, with the high selectivity to fat taste substances, the OBP-based biosensor could be used to interpret fat taste from other tastes.

4. Discussions

4.1. Taste of fat

As one of the basic senses of human beings and animals, gustation plays a very significant role in daily life, such as perceiving desired nutrients at the appropriate levels as pleasant, and warning us of toxic substances at harmful levels as unpleasant. Although the widely accepted "primary" tastes were comprised of sweet, sour, bitter, salty, and umami, the inborn attraction of mammals for fatty foods raised the possibility of an additional oral sensory modality, which might be the fat perception. The mechanisms for fat taste substances accessing to taste receptors might be through forming micelles and binding to some soluble proteins, such as lipocalin-1, which was also known as tear lipocalin, or von Ebner's gland protein [41,44]. Moreover, with multiple candidate receptors (such as CD36 and GPR120) and ion channels (DRK channels) for fat taste stimuli were identified, there might be the sixth basic taste: fat taste, which was even proposed as the term of "oleogustus" [23,27,28].

Actually, the perception of fats for humans and rodents might be dependent on a combination of textural, olfactory, thermal, and gustatory modalities [22]. In order to verify that if gustation played an important role in the detection of fats, especially in free fatty acid detection, researches that utilizing anosmic animals were conducted, which suggested that mice could recognize dietary fat and fatty acid solutions in the oral cavity without any olfactory or textural cues [25,38,45]. More importantly, studies showed that although dietary fats mainly consist of triglycerides, they also contained free fatty acids in concentrations ranging up to 1–3%, among which medium-, and long-chain fatty acids appeared to be responsible for the oral fat perception [23,26,30]. While, fatty acids with less than 10 carbon chain length may cause sour taste that was quite different from the taste of fat [22,46], which was in accordance with the results of this study.

4.2. Fat taste sensing with OBP-based biosensor

For fat taste sensing, early experiments revealed that lipocalin-1 might function as necessary cofactors in gustatory transduction by concentrating and delivering them to the taste receptors. Moreover, binding affinities of lipocalin-1 to fatty acids increased with alkyl chain length increasing [39,41,44]. For human OBPs that also belong to lipocalin superfamily, they shared a common three-dimensional structure with lipocalin-1, and could transport or store biological compounds that were either low solubility or chemically sensitive. Therefore, the structure homology of the OBPs to lipocalin-1 offered a promising opportunity for this kind of OBPs to detect fat taste substances.

Based on the properties of OBPs that have a high affinity to fatty acids, a gustatory biosensor with human OBP II a modified screen-printed electrodes was fabricated for fat taste sensing. In the study, fat taste substances with different lengths of carbon chains were tested, such as docosahexaenoic acid, linoleic acid, and lauric acid. Based on that the hydrophobic cavity of OBPs was the main place for binding different molecules, fatty acids bind to OBP II a might through hydrogen bonds, hydrophobic interactions, and van der waals forces [16,20], which might have great influences on their interactions. Meanwhile, previous studies suggested that the degree of binding energy between lipocalins and fatty acids was related to the number of CH_2 groups in the hydrocarbon tail that extended in the hydrophobic cavities of lipocalins [39–41]. It was likely that the carboxylic acid head of fatty acids oriented toward the exterior solvent and the tail extended into the interior cavity of the protein. Therefore, with the carbon chain length extending, the binding affinity increased until the cavity was filled. Moreover, concerted dynamic phenomena of OBPs conformation might occur when binding to fatty acids, especially those with long chains [21], which could also change electrical properties of the OBPs modified electrodes and decrease the detected cathodic and anodic peak currents. The CV results were in accordance with that OBP II a might bind the long-chain fatty acids more efficiently [20,47]. Thus, the gustatory biosensor had a great potential in evaluating fat taste with different sensitivities.

For fatty acids detection, except the widely used gas chromatography-mass spectrometer (GC–MS), different bio-sensing elements had also been investigated, including cell, yeast, receptors, lipoxygenase, and so on [48–54]. Combined with different detection methods, such as fluorescence, surface plasmon resonance, and amperometric detection, these bio-sensing elements could sensitively detect medium- and long-chain fatty acids (Table 1). For example, through Förster resonance energy transfer (FRET), the detection limit of oleic acid was as low as 10 nM. Comparing to the existing methods for fatty acid detection, the

Table 1
Comparisons between different methods for fatty acid detection.

Method	Sensing element	Fatty acid	Tested concentration	Detection limit	Reference
Immunocytochemical detection	Mouse CD36-positive Gustatory Cells	Linoleic acid	20 μM	–	[48]
Fluorescence detection	Yeast with G-protein coupled receptors	Decanoic acid;	34–250 μM or 110–500 μM;	–	[49]
	Fatty acid binding protein labeled with acrylodan	Oleic acid	0.02–4.7 μmol	0.02 μmol	[50]
Förster resonance energy transfer	Fluorescent dye labeled BSA and quantum dots CdSe/ZnS capped with 3-mercaptopropionic acid	Oleic acid	10–1000 nM.	10 nM	[51]
Surface plasmon resonance	Human p53 DNA binding domain	Docosanoic acid; cis-12-heneicosenoic acid	1.25–10 μM;	–	[52]
Amperometric enzyme sensor	Lipoxygenase	Linoleic acid, a-linolenic acid	0–6 mM	4.9–14 μM; 4.8–14 μM	[53]
Differential pulse voltammetry	15-lipoxygenase	Linoleic acid; Arachidonic acid; Linolenic acid	55–150 μM; 66–110 μM; 140–260 μM	–	[54]
Cyclic voltammetry	Human odorant-binding proteins	Lauric acid; Linoleic acid; Docosahexaenoic acid	10^{-9}-10^{-4} mg/ml	10^{-9} mg/ml; 10^{-10} mg/ml; $6*10^{-11}$ mg/ml	This study

OBP-based biosensor with cyclic voltammetry showed a relatively road tested concentration ranges and a lower detection limit.

Studies showed that OBPs had relatively broad binding spectra to the different hydrophobic molecules. For human OBP II a, it showed high affinities to two kinds of hydrophobic molecules, aldehyde compounds (such as benzaldehyde) and medium- and long-chain fatty acids. Cyclic voltammograms of oleic acid at different concentrations were also detected, peak current changes of which were less than 10 μA (Fig. A8). It indicated that human OBP II a cannot specific bind oleic acid. However, interactions between OBPs and hydrophobic molecules were quite different, which could be reflected by the molecule binding affinities. In order to recognize hydrophobic molecules specifically, the binding affinities between OBP and the target molecules should be first determined. In addition, with the help of computer-aided technology, such as molecular docking, binding affinities could also be analyzed for specifically recognizing different hydrophobic molecules [55].

4.3. Applications of the fat taste biosensing

Generally, as one of the most important olfactory proteins in human olfaction, OBP II a played a significant role in transport, storage, or sequestration of a variety of small hydrophobic molecules. Nevertheless, except for identifying in nasal tissues to make sense of smell, OBP II a were also found as the extracellular carriers of lipophilic molecules in several other organs, such as salivary glands [18,19]. It might have correlations with oral chemosensory detection of fat taste substances. Meanwhile, researches showed that OBPs were promising sensing materials because they could not only be expressed and purified easily, but also were highly stable to temperature, solvents, and proteases [16,56,57]. It indicated that this OBP-based biosensor would provide a good platform for fat taste sensing.

As an essential component of normal food intake of humans, fat (lipid) could be sensing in oral cavity to form a flavor perception of foods and even trigger multiple important physiological responses, such as absorption and metabolism of essential nutrients [30,58]. The low efficiency of dietary fatty acid intake and absorption might lead to impaired vision, growth retardation, and reduced learning ability. However, over-consumption of fat could increase the risk of morbidities, such as obesity, diabetes and even cancer. Inspired by other taste biosensors about sour, sweet, bitter, salty, and umami, fat sensing systems showed a promising potential in food and beverage industry, and even in disease diagnostics.

More importantly, humans seem to have an adaptive taste system. That is, upon prolonged exposure to a high-fat diet, the oral gustatory sensing of fat exhibited reduced sensitivities [30]. Therefore, it was important to detect low concentrations of fat taste substances to control the dietary fat and characterize what degree oral fat perception influenced food choice. However, there was still a gap between the standard substance detection and real sample detection. Compared with standard substances, the real samples were quiet complex, which may consist of various components. Therefore, much efforts still should be made to optimize the sensing platform. Through investigating the binding affinities of OBP II a to fatty acids with different alkyl chain lengths, this gustatory biosensor offered an opportunity to evaluate the fat perception, which could be used for food product choice and development, and even for clinical practices.

5. Conclusion

In summary, based on interactions between medium- and long-chain fatty acids and human OBP II a, a gustatory biosensor for fat taste detection was developed with reduced graphene oxide modified screen-printed electrodes. Through detecting fat taste substances that with different alkyl chain lengths, such as docosahexaenoic acid, linoleic acid, and lauric acid, the OBP-based gustatory biosensor showed high sensitivity and specificity to fat taste. It offered a novel platform for fat taste evaluation in the food and beverage industry, and even in health promotion and disease managements.

Acknowledgments

This work was supported by the National Natural Science Foundation of China (Grant No. 31671007) and the Collaborative Innovation Center of Traditional Chinese Medicine Health Management of Fujian province of China.

Appendix A. Supplementary data

Supplementary data associated with this article can be found, in the online version, at http://dx.doi.org/10.1016/j.snb.2017.06.100.

References

[1] P.A. Breslin, An evolutionary perspective on food and human taste, Curr. Biol. 23 (2013) R409–R418.
[2] N. Chaudhari, S.D. Roper, The cell biology of taste, J. Cell Biol. 190 (2010) 285–296.
[3] Q. Liu, F. Zhang, D. Zhang, N. Hu, K.J. Hsia, P. Wang, Extracellular potentials recording in intact taste epithelium by microelectrode array for a taste sensor, Biosens. Bioelectron. 43 (2013) 186–192.
[4] P. Wang, Q. Liu, Y. Xu, H. Cai, Y. Li, Olfactory and taste cell sensor and its applications in biomedicine, Sensor Actuat. A: Phys. 139 (2007) 131–138.
[5] Q. Liu, D. Zhang, F. Zhang, Y. Zhao, K.J. Hsia, P. Wang, Biosensor recording of extracellular potentials in the taste epithelium for bitter detection, Sens. Actuators, B 176 (2013) 497–504.
[6] Q. Liu, F. Zhang, D. Zhang, N. Hu, H. Wang, K.J. Hsia, P. Wang, Bioelectronic tongue of taste buds on microelectrode array for salt sensing, Biosens. Bioelectron. 40 (2013) 115–120.
[7] K. Woertz, C. Tissen, P. Kleinebudde, J. Breitkreutz, Taste sensing systems (electronic tongues) for pharmaceutical applications, Int. J. Pharm. 417 (2011) 256–271.
[8] A. Riul Jr., C.A. Dantas, C.M. Miyazaki, O.N. Oliveira Jr., Recent advances in electronic tongues, Analyst 135 (2010) 2481–2495.
[9] G.-H. Hui, P. Ji, S.-S. Mi, S.-P. Deng, Electrochemical impedance spectrum frequency optimization of bitter taste cell-based sensors, Biosens. Bioelectron. 47 (2013) 164–170.
[10] J. Pevsner, R.R. Reed, P.G. Feinstein, S.H. Snyder, Molecular cloning of odorant-binding protein: member of a ligand carrier family, Science 241 (1988) 336–339.
[11] B.S. Hansson, M.C. Stensmyr, Evolution of insect olfaction, Neuron 72 (2011) 698–711.
[12] H. Venthur, A. Mutis, J.J. Zhou, A. Quiroz, Ligand binding and homology modelling of insect odorant-binding proteins, Physiol. Entomol. 39 (2014) 183–198.
[13] P. Pelosi, R. Mastrogiacomo, I. Iovinella, E. Tuccori, K.C. Persaud, Structure and biotechnological applications of odorant-binding proteins, Appl. Microbiol. Biotechnol. 98 (2014) 61–70.
[14] S. Sankaran, L.R. Khot, S. Panigrahi, Biology and applications of olfactory sensing system: a review, Sens. Actuators, B 171 (2012) 1–17.
[15] M. Larisika, C. Kotlowski, C. Steininger, R. Mastrogiacomo, P. Pelosi, S. Schütz, S.F. Peteu, C. Kleber, C. Reiner-Rozman, C. Nowak, Electronic olfactory sensor based on A. mellifera odorant-binding protein 14 on a reduced graphene oxide field-Effect transistor, Angew. Chem. 127 (2015) 13443–13446.
[16] Y. Lu, D. Zhang, Q. Zhang, Y. Huang, S. Luo, Y. Yao, S. Li, Q. Liu, Impedance spectroscopy analysis of human odorant binding proteins immobilized on nanopore arrays for biochemical detection, Biosens. Bioelectron. 79 (2016) 251–257.
[17] M.Y. Mulla, E. Tuccori, M. Magliulo, G. Lattanzi, G. Palazzo, K. Persaud, L. Torsi, Capacitance-modulated transistor detects odorant binding protein chiral interactions, Nat. Commun. 6 (2015).
[18] A. Schiefner, R. Freier, A. Eichinger, A. Skerra, Crystal structure of the human odorant binding protein, OBPIIa, Proteins Struct. Funct. Bioinf. 83 (2015) 1180–1184.
[19] A. Schiefner, A. Skerra, The menagerie of human lipocalins: a natural protein scaffold for molecular recognition of physiological compounds, Acc. Chem. Res. 48 (2015) 976–985.
[20] L. Briand, C. Eloit, C. Nespoulous, V. Bézirard, J.-C. Huet, C. Henry, F. Blon, D. Trotier, J.-C. Pernollet, Evidence of an odorant-binding protein in the human olfactory mucus: location, structural characterization, and odorant-binding properties, Biochemistry 41 (2002) 7241–7252.
[21] L. Tcatchoff, C. Nespoulous, J.-C. Pernollet, L. Briand, A single lysyl residue defines the binding specificity of a human odorant-binding protein for aldehydes, FEBS Lett. 580 (2006) 2102–2108.
[22] E. Dransfield, The taste of fat, Meat Sci. 80 (2008) 37–42.
[23] F. Laugerette, D. Gaillard, P. Passilly-Degrace, I. Niot, P. Besnard, Do we taste fat? Biochimie 89 (2007) 265–269.
[24] R.D. Mattes, Accumulating evidence supports a taste component for free fatty acids in humans, Physiol. Behav. 104 (2011) 624–631.
[25] A. Chalé-Rush, J.R. Burgess, R.D. Mattes, Evidence for human orosensory (taste?) sensitivity to free fatty acids, Chem. Senses 32 (2007) 423–431.
[26] R.D. Mattes, Oral detection of short-, medium-, and long-chain free fatty acids in humans, Chem. Senses 34 (2009) 145–150.
[27] R.S. Keast, A. Costanzo, Is fat the sixth taste primary? evidence and implications, Flavour 4 (2015) 1.
[28] C.A. Running, B.A. Craig, R.D. Mattes, Oleogustus: the unique taste of fat, Chem. Senses 40 (2015) 507–516.
[29] T.A. Gilbertson, L. Liu, D.A. York, G.A. Bray, Dietary fat preferences are inversely correlated with peripheral gustatory fatty acid Sensitivitya, Ann. N. Y. Acad. Sci. 855 (1998) 165–168.
[30] D. Liu, N. Archer, K. Duesing, G. Hannan, R. Keast, Mechanism of fat taste perception: association with diet and obesity, Prog. Lipid Res. 63 (2016) 41–49.
[31] J.E. Stewart, C. Feinle-Bisset, M. Golding, C. Delahunty, P.M. Clifton, R.S. Keast, Oral sensitivity to fatty acids, food consumption and BMI in human subjects, Br. J. Nutr. 104 (2010) 145–152.
[32] M. Zhou, Y. Wang, Y. Zhai, J. Zhai, W. Ren, F. Wang, S. Dong, Controlled synthesis of large-area and patterned electrochemically reduced graphene oxide films, Chem. Eur. J. 15 (2009) 6116–6120.
[33] L. Chen, Y. Tang, K. Wang, C. Liu, S. Luo, Direct electrodeposition of reduced graphene oxide on glassy carbon electrode and its electrochemical application, Electrochem. Commun. 13 (2011) 133–137.
[34] Y. Zhang, X. Xiao, Y. Sun, Y. Shi, H. Dai, P. Ni, J. Hu, Z. Li, Y. Song, L. Wang, Electrochemical deposition of nickel nanoparticles on reduced graphene oxide film for nonenzymatic glucose sensing, Electroanalysis 25 (2013) 959–966.
[35] L. Yang, D. Liu, J. Huang, T. You, Simultaneous determination of dopamine, ascorbic acid and uric acid at electrochemically reduced graphene oxide modified electrode, Sens. Actuators, B 193 (2014) 166–172.
[36] H. Sampath, J.M. Ntambi, Polyunsaturated fatty acid regulation of genes of lipid metabolism, Annu. Rev. Nutr. 25 (2005) 317–340.
[37] C.A. Running, R.D. Mattes, Humans are more sensitive to the taste of linoleic and alpha-linolenic than oleic acid, Am. J. Physiol. Gastrointest. Liver Physiol. 308 (2015) G442–G449.
[38] K. Saitou, T. Yoneda, T. Mizushige, H. Asano, M. Okamura, S. Matsumura, A. Eguchi, Y. Manabe, S. Tsuzuki, K. Inoue, Contribution of gustation to the palatability of linoleic acid, Physiol. Behav. 96 (2009) 142–148.
[39] A.R. Abduragimov, O.K. Gasymov, T.N. Yusifov, B.J. Glasgow, Functional cavity dimensions of tear lipocalin, Curr. Eye Res. 21 (2000) 824–832.
[40] O.K. Gasymov, A.R. Abduragimov, T.N. Yusifov, B.J. Glasgow, Binding studies of tear lipocalin: the role of the conserved tryptophan in maintaining structure, stability and ligand affinity, Biochim. Biophys. Acta, Protein Struct. Mol. Enzymol. 1433 (1999) 307–320.
[41] R.M. Tucker, R.D. Mattes, C.A. Running, Mechanisms and effects of fat taste in humans, Biofactors 40 (2014) 313–326.
[42] S. Zubkov, A.M. Gronenborn, I.-J.L. Byeon, S. Mohanty, Structural consequences of the pH-induced conformational switch in A. polyphemus pheromone-binding protein: mechanisms of ligand release, J. Mol. Biol. 354 (2005) 1081–1090.
[43] N.R. Leite, R. Krogh, W. Xu, Y. Ishida, J. Iulek, W.S. Leal, G. Oliva, Structure of an odorant-binding protein from the mosquito Aedes aegypti suggests a binding pocket covered by a pH-sensitive Lid, PLoS One 4 (2009) e8006.
[44] H. Schmale, H. Holtgreve-Grez, H. Christiansen, Possible Role for Salivary Gland Protein in Taste Reception Indicated by Homology to Lipophilic-ligand Carrier Proteins, 1990.
[45] T. Fukuwatari, K. Shibata, K. Iguchi, T. Saeki, A. Iwata, K. Tani, E. Sugimoto, T. Fushiki, Role of gustation in the recognition of oleate and triolein in anosmic rats, Physiol. Behav. 78 (2003) 579–583.
[46] D.A. Forss, Odor and flavor compounds from lipids, Prog. Chem. Fats Other Lipids 13 (1973) 177–258.
[47] Y. Lu, Y. Yao, Q. Zhang, D. Zhang, S. Zhuang, H. Li, Q. Liu, Olfactory biosensor for insect semiochemicals analysis by impedance sensing of odorant-binding proteins on interdigitated electrodes, Biosens. Bioelectron. 67 (2015) 662–669.
[48] A. El-Yassimi, A. Hichami, P. Besnard, N.A. Khan, Linoleic acid induces calcium signaling, Src kinase phosphorylation, and neurotransmitter release in mouse CD36-positive gustatory cells, J. Biol. Chem. 283 (2008) 12949–12959.
[49] K. Mukherjee, S. Bhattacharyya, P. Peralta-Yahya, GPCR-based chemical biosensors for medium-chain fatty acids, ACS Synth. Biol. 4 (2015) 1261–1269.
[50] A. Bartolome, C. Bardliving, G. Rao, L. Tolosa, Fatty acid sensor for low-cost lifetime-assisted ratiometric sensing using a fluorescent fatty acid binding protein, Anal. Biochem. 345 (2005) 133–139.
[51] S.V. Dezhurov, I.Y. Volkova, M.S. Wakstein, FRET-based biosensor for oleic acid in nanomolar range with quantum dots as an energy donor, Bioconjugate Chem. 22 (2011) 338–345.
[52] H. Iijima, N. Kasai, H. Chiku, S. Murakami, F. Sugawara, K. Sakaguchi, H. Yoshida, Y. Mizushina, The inhibitory action of long-chain fatty acids on the DNA binding activity of p53, Lipids 41 (2006) 521–527.
[53] M. Schoemaker, R. Feldbrügge, B. Gründig, F. Spener, The lipoxygenase sensor, a new approach in essential fatty acid determination in foods, Biosens. Bioelectron. 12 (1997) 1089–1099.
[54] A. Rittmannsberger, W. Likussar, A. Michelitsch, Development of an enzyme-modified carbon paste electrode for determining inhibitors of lipoxygenase, Biosens. Bioelectron. 21 (2005) 655–660.
[55] Y. Zhang, I-TASSER server for protein 3D structure prediction, BMC Bioinf. 9 (2008) 40.
[56] Y. Hou, N. Jaffrezic-Renault, C. Martelet, C. Tlili, A. Zhang, J.-C. Pernollet, L. Briand, G. Gomila, A. Errachid, J. Samitier, Study of Langmuir and Langmuir-Blodgett films of odorant-binding protein/amphiphile for odorant biosensors, Langmuir 21 (2005) 4058–4065.
[57] Y. Wei, A. Brandazza, P. Pelosi, Binding of polycyclic aromatic hydrocarbons to mutants of odorant-binding protein: a first step towards biosensors for environmental monitoring, Biochim. Biophys. Acta, Proteins Proteomics 1784 (2008) 666–671.
[58] C.A. Running, R.D. Mattes, R.M. Tucker, Fat taste in humans: sources of within-and between-subject variability, Prog. Lipid Res. 52 (2013) 438–445.

Biographies

Yanli Lu received her bachelor degree in Xi'an Jiaotong University in 2012. Now she is a Ph.D. student of biomedical engineering of Zhejiang University. Her work includes OBPs-based biosensors and electronic measurement.

Yixuan Huang received her bachelor degree in Zhejiang University in 2016. Now she is a master student of bioengineering of the University of Tokyo. Her work includes biosensors and biocompatible sensing materials.

Shuang Li received her bachelor degree in Hunan normal University in 2014. Now she is a Ph.D. student of biomedical engineering of Zhejiang University. Her work includes biosensors and electronic measurement.

Qian Zhang received her bachelor degree in Zhejiang University in 2012. Now she is a Ph.D. student of biomedical engineering of Zhejiang University. Her work includes biosensors and electronic measurement.

Jiajia Wu received his bachelor degree in Zhejiang University in 2016. Now she is a Ph.D. student of biomedical engineering of Zhejiang University. Her work includes biosensors and electronic measurement.

Zhongyan Xiong is an undergraduate student of biomedical engineering of Zhejiang University. Her work includes biosensors and electronic measurement.

Lingxi Xiong is an undergraduate student of biomedical engineering of Zhejiang University. Her work includes biosensors and electronic measurement.

Qianqian Wan is an undergraduate student of biomedical engineering of Zhejiang University. Her work includes biosensors and electronic measurement.

Qingjun Liu received his Ph.D. degree in biomedical engineering from Zhejiang University, PR China in 2006. He is currently a professor in Biosensor National Special Laboratory, Zhejiang University. He is also a visiting scholar in the Micro and Nanotechnology Laboratory (MNTL) at the University of Illinois at Urbana-Champaign (UIUC). He published the book of Cell-Based Biosensors: Principles and Applications, by Artech House Publishers USA in October 2009. His research interests concentrate on the biosensors (e.g. living cell sensor, DNA sensor and protein sensor) and BioMEMS system.